

# Spectral signature of cosmological infall of gas around the first quasars

Rennan Barkana\* & Abraham Loeb†‡

\* School of Physics and Astronomy, Tel Aviv University, Tel Aviv 69978, Israel  
 † Astronomy Department, Harvard University, Cambridge, Massachusetts 02138, USA

Recent observations have shown that, only a billion years after the Big Bang, the Universe was already lit up by bright quasars<sup>1</sup> fuelled by the infall of gas onto supermassive black holes. The masses of these early black holes are inferred from their luminosities to be  $>10^9$  solar masses ( $M_{\odot}$ ), which is a difficult theoretical challenge to explain. Like nearby quasars, the early objects could have formed in the central cores of massive host galaxies. The formation of these hosts could be explained if, like local large galaxies, they were assembled gravitationally inside massive ( $>10^{12} M_{\odot}$ ) haloes of dark matter<sup>2</sup>. There has hitherto been no observational evidence for the presence of these massive hosts or their surrounding haloes. Here we show that the cosmic gas surrounding each halo must respond to its strong gravitational pull, where absorption by the infalling hydrogen produces a distinct spectral signature. That signature can be seen in recent data<sup>3,4</sup>.

We model the effect of resonant Lyman  $\alpha$  absorption by infalling gas on the quasar light (Fig. 1). For each quasar we consider the history of the formation of its host halo from an initial positive overdensity of dark matter. For the initial surrounding density profile at high redshift we adopt the typical profile expected around the dense region that collapses to form the halo<sup>5</sup>. This profile, as well as the approximation of a spherical geometry, are particularly satisfactory for the very rare and massive haloes under consideration. We calculate gas infall down to the radius of the accretion shock, and neglect any Ly $\alpha$  absorption due to the post-shock gas. The hot ( $\approx 10^7$  K) post-shock gas should be fully ionized by collisions. Part of it is expected to subsequently cool and collapse onto the galactic disk, but Compton heating by the quasar should keep the virialized gas hotter than about  $10^6$  K. Even if a thin cold shell of shocked gas remains, it will not change the basic pattern produced by infalling gas because the post-shock gas no longer has a high infall velocity.

In order to predict the Ly $\alpha$  absorption around a quasar we must estimate the mass of its host halo. A tight correlation has been measured in local galaxies between the mass of the central black hole and the bulge velocity dispersion<sup>6,7</sup>. This relation also fits all existing data on the luminosity function of high-redshift quasars within a simple model<sup>8</sup> in which quasar emission is assumed to be triggered by mergers during hierarchical galaxy formation. We use the best-fit<sup>6-8</sup> relation, in which the black hole mass ( $M_{\text{BH}}$ ) in multiples of  $10^8 M_{\odot}$  is related to the circular velocity ( $V$ ) at the halo boundary in multiples of  $300 \text{ km s}^{-1}$  by  $M_{\text{BH}} = 1.5V^5$ . For the typical quasar continuum spectrum, we adopt a power-law spectral flux shape of  $F_{\nu} \propto \nu^{-0.44}$  in the rest-frame range  $1,190\text{--}5,000 \text{ \AA}$ , based on the Sloan Digital Sky Survey (SDSS) composite spectrum<sup>9</sup>, and  $F_{\nu} \propto \nu^{-1.57}$  at  $500\text{--}1,190 \text{ \AA}$ , using the composite quasar spectrum from the Hubble Space Telescope<sup>10</sup>. On the basis of observations in soft X-rays<sup>11</sup>, we extend this power-law towards short wavelengths.

We assume that the brightest quasars shine at their Eddington luminosity, and we note that for the SDSS composite spectrum<sup>9</sup>, the total luminosity above  $1,190 \text{ \AA}$  equals 1.6 times the total continuum luminosity at  $1,190\text{--}5,000 \text{ \AA}$ . Thus, ionizing photons stream out of the quasar's galactic host at the rate  $\dot{N} = 1.04 \times 10^{56} M_{\text{BH}} \text{ s}^{-1}$ . We

infer the black hole mass using the observed continuum at  $1,350 \text{ \AA}$ , with the conversion  $F_{\nu} = 1.74 \times 10^{30} M_{\text{BH}} \text{ erg s}^{-1} \text{ Hz}^{-1}$ . Given that helium is doubly ionized by the quasar, the frequency-averaged photoionization cross-section of hydrogen is, for our template spectrum,  $\sigma_{\text{H}} = 2.3 \times 10^{-18} \text{ cm}^2$ . The double ionization of helium increases the recombination rate owing to the extra electrons, and also produces a characteristic gas temperature of around  $1.5 \times 10^4 \text{ K}$  in regions that have already been reionized by a softer ionizing background<sup>12</sup>.

Only a limited number of published spectra are currently available for a clear test of our predictions. First, only the brightest quasars, which reside in the most massive haloes, produce strong infall over a large surrounding region. The infalling gas density scales as  $(1+z)^3$  and the shock radius scales as  $(1+z)^{-1}$ , so that the absorption optical depth (see below) scales roughly as  $(1+z)^4$  and the absorption feature is much weaker at low redshift. Even at high redshifts, measuring the detailed Ly $\alpha$  line profile is possible only in a high-resolution spectrum with an extremely high signal-to-noise ratio.

Figure 2 shows two particularly high-quality spectra and compares them with our model predictions. Both spectra show our predicted double-peak pattern and disagree with the single-peaked profile predicted by previous models that ignored infall. In particular,

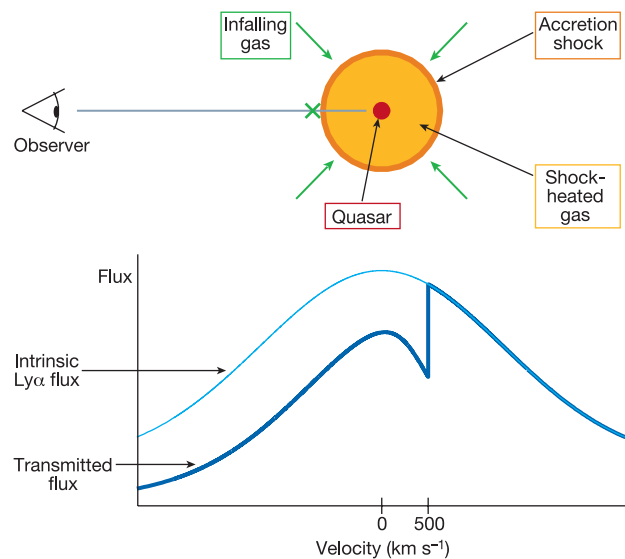


**Figure 1** Schematic illustration of how infall produces a unique spectral signature. A quasar forms inside a galaxy that lies at the centre of a massive dark matter halo. A large volume of gas responds to the strong gravitational pull and falls towards the massive halo. As infalling gas impacts on the galactic gas, a strong accretion shock forms. The intrinsic quasar Lyman  $\alpha$  emission is partially absorbed by the infalling pre-shock gas. In particular, a sharp flux drop is caused by gas (marked with a cross) that is about to hit the accretion shock. This gas is falling towards the quasar at  $500 \text{ km s}^{-1}$  in this sketch. We calculate spherically symmetric infall<sup>17</sup> and set the accretion shock radius to 1.15 times the halo boundary<sup>18</sup>, although our results are not altered substantially as long as the shock radius is close to the halo virial radius. Three-dimensional hydrodynamic simulations show that the most massive haloes at any time in the universe are indeed surrounded by strong, quasi-spherical accretion shocks<sup>19,20</sup>. Preliminary evidence has been found for such shocks around nearby galaxy clusters<sup>21,22</sup>. We model resonant Ly $\alpha$  absorption by intergalactic hydrogen<sup>23</sup> that is partially ionized by the radiation produced by the quasar<sup>24</sup>. In addition to the overall infall pattern<sup>5</sup> we include a realistic distribution of gas density fluctuations<sup>25</sup>. For the distribution of gas clumps we adopt an analytical fit to numerical simulations<sup>26</sup>. We assume that the clumps are optically thin, and find the neutral fraction separately for each clumping density based on ionization equilibrium with the quasar ionizing flux. We then calculate the mean Ly $\alpha$  transmission averaged over the clump distribution. Note that the absorbed Ly $\alpha$  photons are re-emitted from a large Ly $\alpha$  halo<sup>27,28</sup> that is too faint to significantly affect current observations.

‡ Present address: Institute for Advanced Study, Princeton, New Jersey 08540, USA.

models that assume a pure Hubble flow firmly predict no absorption at all at positive velocities and only a gradual decline in the transmitted flux toward negative velocities. This slow decline is due to the fact that in these models the gas closest to the quasar produces no absorption because it is fully ionized by the strong ionizing intensity of the quasar. More distant gas recedes along with the universal expansion and absorbs only at negative velocities. Our model, in contrast, firmly predicts a sharp flux cutoff located at a positive velocity. This flux drop corresponds to absorption by gas just outside the accretion shock, and the positive velocity of the cutoff corresponds to the infall velocity. The strong absorption caused by this gas, despite exposure to the ionizing flux from the quasar, is due to the high density of the infalling gas. This gas is expected to be about 10–30 times denser than the cosmic mean after having fallen toward the quasar host halo over the history of its formation.

The infall velocity is proportional to the halo circular velocity and thus<sup>2</sup> to  $M^{1/3}(1+z)^{3/2}$ , in terms of the halo mass  $M$  and the redshift  $z$ . The actual physical distance of the accretion shock in the model is 86 kpc and 80 kpc for the quasars at  $z = 4.795$  and  $z = 6.28$ , respectively. Our model with infall also fits approximately the secondary peak that is observed on the blue side of the main peak (that is, at lower velocity). This blue peak corresponds closely to the point of weakest absorption by the infalling gas, although the profile of the intrinsic quasar emission also affects the precise location of this peak. In this region we do not expect to fit the flux profile in full detail; our model averages over all lines of sight and possible quasar positions, but observable random fluctuations around our predicted mean are expected in each specific spectrum.

However, once we average over the density fluctuations, the prediction of a second peak rather than a smooth fall-off is generic and insensitive to the detailed model assumptions. At a distance  $R$  from the quasar the resonant optical depth depends on  $\rho^2 R^2$ , where  $\rho$  is the density including infall; one factor of  $\rho$  comes from the total gas density, the second comes from the H I fraction which increases with  $\rho$  owing to recombinations, and the  $R$ -dependence results from the  $R^{-2}$  decline of the ionizing intensity of the quasar. Thus, a second peak should appear as long as infall produces a density profile falling off faster than  $1/R$  (our model predicts  $R^{-3/2}$ ) before asymptotically tending to the cosmic mean value of unity. We note that in our model the position of the blue peak corresponds to absorption by gas at  $R = 0.45$  Mpc ( $z = 4.795$ ) or  $0.41$  Mpc ( $z = 6.28$ ).

Even in each particular spectrum, the more distant region where the flux drops toward zero can be modelled much more robustly. In particular, significant flux is observed at  $\Delta V = -2,000$  km s<sup>-1</sup> ( $z = 4.795$ ) and  $\Delta V = -3,000$  km s<sup>-1</sup> ( $z = 6.28$ ), respectively. These relatively distant regions are only weakly affected by infall and the observed positions translate to a distance from the quasar of 3.8 Mpc ( $z = 4.795$ ) or 4.2 Mpc ( $z = 6.28$ ). In models that do not include a clump distribution, the optical depth at these positions is  $\geq 3$ , which means that the observed flux requires an intrinsic unabsorbed flux that is 20 times greater. This is clearly impossible, regardless of any uncertainties about the intrinsic line shape and the quasar continuum level. To explain the observed flux, the ionizing intensity of the quasar as determined by our template spectrum from the observed continuum would have to be too low by a factor greater than 2. However, our full model accounts for the fact that part of the cosmic gas falls into dense sheets and filaments and leaves the rest with a density below the cosmic mean. The resonant Ly $\alpha$  absorption is made up of the separate contributions of gas elements at a variety of overdensities, and because gas in low-density regions absorbs very weakly, clumping actually increases the mean transmission. Thus, our model naturally accounts for the flux observed far from the quasar, with no change required in the quasar spectrum.

Our conclusions are insensitive to the question of whether the

H II region of the highest redshift quasar is surrounded by a region of neutral hydrogen (owing to the fact that the universe had not been fully reionized by  $z = 6.28$  (ref. 13)) or not<sup>14</sup>; a distant neutral region would only add on the intergalactic medium damping wing<sup>15</sup>, which produces a smooth, gradual suppression that should not alter the basic double-peak pattern. We note that the quasar may possess a velocity offset relative to Hubble flow owing, for example, to a violent galactic merger that had originally activated the quasar. However, the close fit that we find between the predicted accretion shock position and the observed flux drop is evidence against the presence of a large velocity offset in the two quasars we have considered. We also note that if the observed absorption pattern were due to dense gas clouds within the galaxy (for example, in the region feeding the central black hole), then the absorbing gas would be expected to contain heavy elements such as carbon, oxygen and nitrogen. This gas would then be expected to absorb other emission lines of the quasar in addition to Ly $\alpha$ . Such associated absorption is absent in the  $z = 4.795$  quasar which has several emission lines with

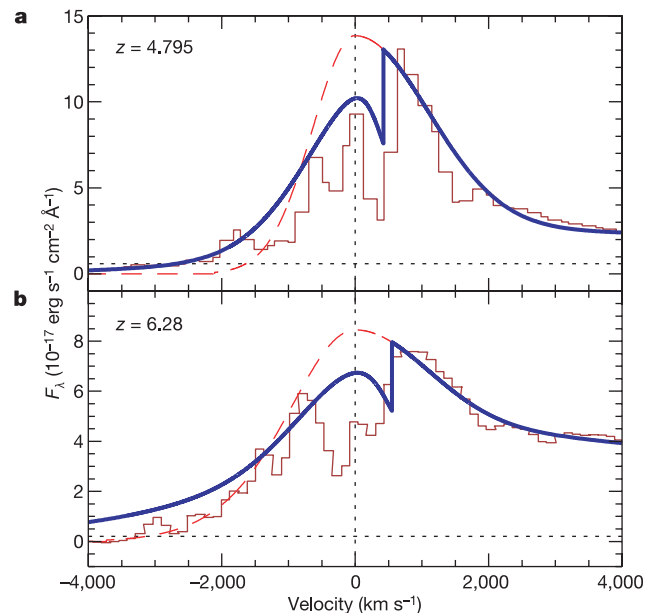


**Figure 2** Comparison between models of cosmological infall and observed quasar spectra. **a**, The redshift  $4.795 \pm 0.004$  quasar SDSS1122–0229 (ref. 3); on the basis of observed redshift and continuum level our model implies a  $4.6 \times 10^8 M_{\odot}$  black hole residing in a  $2.5 \times 10^{12} M_{\odot}$  host halo. **b**, The redshift  $6.28 \pm 0.02$  quasar SDSS1030 + 0524 (ref. 4), for which our model implies a  $1.9 \times 10^9 M_{\odot}$  black hole residing in a  $4.0 \times 10^{12} M_{\odot}$  host halo (we do not use a second spectral observation of this source<sup>29</sup> because it appears to have a significantly lower signal-to-noise ratio). In **a** and **b**, the histogram shows the observed spectrum, the dashed line shows previous models that assume a uniform expanding universe, and the solid line shows our model which includes cosmological infall as well as a realistic distribution of gas clumps. Note that the velocity is measured relative to the quasar, where negative velocity means motion towards us. In **a** and **b**, the vertical dotted line shows the position of the Ly $\alpha$  wavelength at the source redshift, and the horizontal dotted line shows the flux level of the highest transmission peaks seen in parts of the spectrum corresponding to the average intergalactic medium (that is, at velocities more negative than  $-4,000$  km s<sup>-1</sup>). We assume an intrinsic emission line given by a sum of two gaussian components, a form which best fits the line shape of most quasars at low redshift<sup>30</sup>; we fix the parameters for each quasar on the basis of the unabsorbed part of the Ly $\alpha$  line at velocities above 500 km s<sup>-1</sup>. With this approach the models do not include any free parameters. Particular quasars are expected to show fluctuations around our predicted absorption profile, because our model averages over random lines of sight and density fluctuations. Throughout this paper we assume the standard cosmological parameters  $\Omega_m = 0.3$ ,  $\Omega_{\Lambda} = 0.7$ ,  $\Omega_b = 0.05$ ,  $H_0 = 70$  km s<sup>-1</sup> Mpc<sup>-1</sup> and  $n = 1$ .  $F_{\lambda}$  is the total energy from the quasar crossing a unit area per second per unit wavelength.

well-measured profiles<sup>3</sup>, suggesting that the absorbing gas has a near-primordial composition as expected for intergalactic gas.

Our models provide direct evidence that two characteristic properties of quasars at low redshift are also applicable to bright quasars in the early Universe. These properties include the quasar spectral template, which determines the ionizing intensity of the quasar, and the relation between black hole mass and halo velocity dispersion, which we have used to determine the host halo mass. Both observed spectra show a blue peak of about 75% of the height of the red (positive velocity) peak, and this is roughly matched by the models. However, if we were to increase the ionizing intensity by an order of magnitude, then we would predict a blue peak at least of equal height to the other peak. If, instead, we decreased the ionizing intensity by an order of magnitude, then the resulting blue peak would be under 50% of the height of the red peak and the transmitted flux would decrease to zero toward negative velocities much faster than is observed. Similarly, if we varied the assumed halo mass by more than an order of magnitude then the resulting absorption profile in each quasar would disagree with the data. High-redshift quasars could in principle be much fainter intrinsically than they appear, if they are magnified by gravitational lensing<sup>16</sup>; our limits on the ionizing intensity, however, suggest that the two quasars we have modelled cannot be magnified by a factor of more than about ten.

We can also estimate from the data the total gas infall rates into these massive galaxies. The positions of the accretion shocks imply, in our models, infall velocities of 400–550 km s<sup>-1</sup> and shock radii of 80–90 kpc. Gas at this radius is expected to have a density of about 20 times the cosmic mean density<sup>5</sup>, so we obtain accretion rates of 1,300 M<sub>⊙</sub> yr<sup>-1</sup> (z = 4.795) and 2,900 M<sub>⊙</sub> yr<sup>-1</sup> (z = 6.28), respectively. At these rates, the host galaxies of these two quasars could have been assembled in (2–3) × 10<sup>8</sup> yr, consistent with the 9 × 10<sup>8</sup> yr age of the Universe at z = 6.28. Future comparison of our model to the average Ly $\alpha$  absorption profile of a statistical sample of bright, early quasars with similar luminosities and redshifts should allow us to fit the details of the absorption spectrum and refine our quantitative conclusions. □

Received 25 September; accepted 26 November 2002; doi:10.1038/nature01330.

1. Fan, X. *et al.* Survey of z > 5.8 quasars in the Sloan digital sky survey. I. Discovery of three new quasars and the spatial density of luminous quasars at z ~ 6. *Astron. J.* **122**, 2833–2849 (2001).
2. Barkana, R. & Loeb, A. In the beginning: the first sources of light and the reionization of the universe. *Phys. Rep.* **349**, 125–238 (2001).
3. Zheng, W. *et al.* Five high-redshift quasars discovered in commissioning imaging data of the Sloan Digital Sky Survey. *Astron. J.* **120**, 1607–1611 (2000).
4. Becker, R. H. *et al.* Evidence for reionization at z ~ 6: Detection of a Gunn-Peterson trough in a z = 6.28 quasar. *Astron. J.* **122**, 2850–2857 (2001).
5. Loeb, A. & Eisenstein, D. J. Probing early clustering with Ly $\alpha$  absorption lines beyond the quasar redshift. *Astrophys. J.* **448**, 17–26 (1995).
6. Ferrarese, L. & Merritt, D. A fundamental relation between supermassive black holes and their host galaxies. *Astrophys. J.* **539**, L9–L12 (2000).
7. Tremaine, S. *et al.* The slope of the black hole mass versus velocity dispersion correlation. *Astrophys. J.* **574**, 740–753 (2002).
8. Wyithe, J. S. B., Loeb, A. A physical model for the luminosity function of high-redshift quasars. *Astrophys. J.* (in the press).
9. Vanden Berk, D. E. *et al.* Composite quasar spectra from the Sloan Digital Sky Survey. *Astron. J.* **122**, 549–564 (2001).
10. Telfer, R. C., Zheng, W., Kriss, G. A. & Davidsen, A. F. The rest-frame extreme-ultraviolet spectral properties of quasi-stellar objects. *Astrophys. J.* **565**, 773–785 (2002).
11. Yuan, W., Brinkmann, W., Siebert, J. & Voges, W. Broad band energy distribution of ROSAT detected quasars. II. Radio-quiet objects. *Astron. Astrophys.* **330**, 108–122 (1998).
12. Abel, T. & Haehnelt, M. G. Radiative transfer effects during photoheating of the intergalactic medium. *Astrophys. J.* **520**, L13–L16 (1999).
13. Fan, X. *et al.* Evolution of the ionizing background and the epoch of reionization from the spectra of z ~ 6 quasars. *Astron. J.* **123**, 1247–1257 (2002).
14. Barkana, R. Did the universe reionize at redshift six? *New Astron.* **7**, 85–100 (2002).
15. Miralda-Escudé, J. Reionization of the intergalactic medium and the damping wing of the Gunn-Peterson trough. *Astrophys. J.* **501**, 15–22 (1998).
16. Wyithe, J. S. B. & Loeb, A. Magnification of light from many distant quasars by gravitational lenses. *Nature* **417**, 923–925 (2002).
17. Gunn, J. E. & Gott, J. R. On the infall of matter into clusters of galaxies and some effects on their evolution. *Astrophys. J.* **176**, 1–19 (1972).
18. Bertschinger, E. Self-similar secondary infall and accretion in an Einstein–de Sitter universe. *Astrophys. J. Suppl.* **58**, 39–65 (1985).

19. Keshet, U., Waxman, E., Loeb, A., Springel, V., Hernquist, L. Gamma-rays from intergalactic shocks. *Astrophys. J.* (in the press).
20. Abel, T., Bryan, G. L. & Norman, M. L. The formation of the first star in the universe. *Science* **295**, 93–98 (2002).
21. Scharf, C. A., Mukherjee, R. A statistical detection of gamma-ray emission from galaxy clusters: implications for the gamma-ray background and structure formation. *Astrophys. J.* **580**, 154–163 (2002).
22. Loeb, A. & Waxman, E. Cosmic  $\gamma$ -ray background from structure formation in the intergalactic medium. *Nature* **405**, 156–158 (2000).
23. Gunn, J. E. & Peterson, B. A. On the density of neutral hydrogen in intergalactic space. *Astrophys. J.* **142**, 1633–1641 (1965).
24. Bajlik, S., Duncan, R. C. & Ostriker, J. P. Quasar ionization of Ly $\alpha$  clouds—the proximity effect, a probe of the ultraviolet background at high redshift. *Astrophys. J.* **327**, 570–583 (1988).
25. Haiman, Z. The detectability of high-redshift Ly $\alpha$  emission lines prior to the reionization of the universe. *Astrophys. J.* **576**, L1–L4 (2002).
26. Miralda-Escudé, J., Haehnelt, M. & Rees, M. J. Reionization of the inhomogeneous universe. *Astrophys. J.* **530**, 1–16 (2000).
27. Loeb, A. & Rybicki, G. B. Scattered Lyman alpha radiation around sources before cosmological reionization. *Astrophys. J.* **524**, 527–535 (1999).
28. Haiman, Z. & Rees, M. J. Extended Lyman alpha emission around young quasars: A constraint on galaxy formation. *Astrophys. J.* **556**, 87–92 (2001).
29. Pentericci, L. *et al.* VLT optical and near-infrared observations of the z = 6.28 quasar SDSS J1030 + 0524. *Astron. J.* **123**, 2151–2158 (2002).
30. Brotherton, M. S., Wills, B. J., Steidel, C. C. & Sargent, W. L. W. Statistics of QSO broad emission-line profiles. 2: The C IV wavelength 1549, C III wavelength 1909, and MG II wavelength 2798 lines. *Astrophys. J.* **423**, 131–142 (1994).

**Acknowledgements** We thank E. Turner and H. Netzer for discussions, and are grateful for the hospitality of the Institute for Advanced Study where this work was completed. R.B. acknowledges the support of an Alon Fellowship at Tel Aviv University and of the Israel Science Foundation. A.L. acknowledges support from the Institute for Advanced Study and a John Simon Guggenheim Memorial Fellowship. This work was also supported by the National Science Foundation.

**Competing interests statement** The authors declare that they have no competing financial interests.

**Correspondence** and requests for materials should be addressed to R.B. (e-mail: barkana@wise.tau.ac.il) or A.L. (e-mail: loeb@ias.edu).

## Experimental extraction of an entangled photon pair from two identically decohered pairs

Takashi Yamamoto\*†, Masato Koashi\*†, Şahin Kaya Özdemir\*† & Nobuyuki Imoto\*†‡

\* School of Advanced Sciences, The Graduate University for Advanced Studies (SOKENDAI), Hayama, Kanagawa, 240-0193, Japan  
 † CREST Interacting Carrier Electronics Project, 4-1-8 Honmachi, Kawaguchi, 331-0012, Japan  
 ‡ NTT Basic Research Laboratories, NTT Corporation, 3-1 Morinosato-Wakamiya, Atsugi, 243-0198, Japan

Entanglement is considered to be one of the most important resources in quantum information processing schemes, including teleportation<sup>1–3</sup>, dense coding<sup>4</sup> and entanglement-based quantum key distribution<sup>5</sup>. Because entanglement cannot be generated by classical communication between distant parties, distribution of entangled particles between them is necessary. During the distribution process, entanglement between the particles is degraded by the decoherence and dissipation processes that result from unavoidable coupling with the environment. Entanglement distillation and concentration schemes<sup>6–9</sup> are therefore needed to extract pairs with a higher degree of entanglement from these less-entangled pairs; this is accomplished using local operations and classical communication. Here we report an experimental demonstration of extraction of a polarization-entangled photon pair from two decohered